



UNIVERSITY OF LEEDS

This is a repository copy of *Tackling Mobility in Low Latency Deterministic Multihop IEEE 802.15.4e Sensor Network*.

White Rose Research Online URL for this paper:  
<http://eprints.whiterose.ac.uk/104557/>

Version: Accepted Version

---

**Article:**

Al-Nidawi, Y, Yahya, H and Kemp, AH (2016) Tackling Mobility in Low Latency Deterministic Multihop IEEE 802.15.4e Sensor Network. *Proceedings of IEEE Sensors*, 16 (5). pp. 1412-1427. ISSN 1530-437X

<https://doi.org/10.1109/JSEN.2015.2500502>

---

(c) 2016 IEEE. This is an author produced version of a paper published in *Proceedings of IEEE Sensors*. Uploaded in accordance with the publisher's self-archiving policy. Personal use of this material is permitted. Permission from IEEE must be obtained for all other users, including reprinting/ republishing this material for advertising or promotional purposes, creating new collective works for resale or redistribution to servers or lists, or reuse of any copyrighted components of this work in other works.

**Reuse**

Unless indicated otherwise, fulltext items are protected by copyright with all rights reserved. The copyright exception in section 29 of the Copyright, Designs and Patents Act 1988 allows the making of a single copy solely for the purpose of non-commercial research or private study within the limits of fair dealing. The publisher or other rights-holder may allow further reproduction and re-use of this version - refer to the White Rose Research Online record for this item. Where records identify the publisher as the copyright holder, users can verify any specific terms of use on the publisher's website.

**Takedown**

If you consider content in White Rose Research Online to be in breach of UK law, please notify us by emailing [eprints@whiterose.ac.uk](mailto:eprints@whiterose.ac.uk) including the URL of the record and the reason for the withdrawal request.



[eprints@whiterose.ac.uk](mailto:eprints@whiterose.ac.uk)  
<https://eprints.whiterose.ac.uk/>

# Tackling Mobility in Low Latency Deterministic Multihop IEEE 802.15.4e Sensor Network

Yaarob Al-Nidawi, *Student Member, IEEE*, Harith Yahya, *Student Member, IEEE*, and Andrew H. Kemp, *Member, IEEE*

**Abstract**—Providing reliable services for low latency (LL) applications within the IoT context is a challenging issue. Several wireless sensor network (WSN) applications require deterministic systems that ensure a reliable and low latency aggregation service. The IEEE 802.15.4e standard, which is considered as the backbone of the IoT regarding WSN, has presented the low-latency deterministic network mode (LLDN) that can fulfil the major requirements of low latency applications. Meanwhile, several LL applications, for example in the automotive industry, demand the support of sensor node mobility which in turn affects network performance. Node mobility triggers several dissociations from the network that will increase latency and degrade node throughput. In this paper, we investigate the impact of node mobility over the LLDN mode while defining key factors that maximize latency and degrade throughput. In addition, an enhanced version of the LLDN mode is presented and evaluated that supports node mobility while maintaining the targeted limits of LL application requirements. The proposed mobility aware (MA-LLDN) technique manages to reduce the dissociation overhead by a factor of 75% while the packet delivery ratio (PDR) has been enhanced by 30%. Furthermore, this paper presents an analytical model that provides a snapshot of the tradeoff process between different metrics in the IEEE 802.15.4e LLDN design, which must be considered prior network deployment in mobile LL applications.

**Index Terms**—Low Latency; IEEE 802.15.4e; LLDN; nodes mobility; Markov chain; multihop.

## I. INTRODUCTION

SEVERAL standardization efforts are collaborating to shape the concept of the internet of things (IoT). Within the WSN field, three standardized elements are merged to facilitate the integration of WSN into the IoT world. These elements are the IEEE 802.15.4 [1], 6LoWPAN [2] adaptation layer and IPv6 protocol [3]. IEEE 802.15.4 here is acting as the backbone of the IoT, from the WSN's perspective, by which it provides the physical and MAC infrastructure of the IoT paradigm. Hence, optimizing the IEEE 802.15.4 standard performance has major advantages that could influence and contribute to the integrity of the IoT functionality. One of the

application types that need to be addressed carefully is the LL applications. These applications must be considered by deterministic systems that ensure minimized latency in order to maintain network reliability and availability. Thus, the IEEE 802.15.4 has presented the LLDN within the first amendment (IEEE 802.15.4e MAC sublayer) [4]. The LLDN objective is to facilitate aggregating data sensor nodes within a time window of no more than 10ms<sup>1</sup>. However, default LLDN mode specifications cannot fit the requirement of all the addressed LL applications due to several constraints. Applications like automotive manufacturing, health applications (wearable sensors [5]), cargo containers [6], remote goods tracking [7], airport logistics and portable machine tools all encompass the mobility feature. Sensor nodes movement within a deployment field needs to be addressed carefully by ensuring two important parameters; (i) full area coverage to ensure the entire sensing area field is covered by multiple coordinators and to eliminate any coverage black holes, (ii) all the nodes must have a reliable, lightweight and fast mobility management scheme that minimizes the required time to associate with a new coordinator.

Under the IoT umbrella, node mobility can be handled by three different approaches based on the network stack layer that will accomplish this task. Hence, it can either be managed through IEEE 802.15.4e, 6LoWPAN or the IPv6 protocol (i.e. MIPv6). Prior to devising the layer that should be assigned to tackle the mobility issue, we have to determine the type of node mobility in order to consider the optimum approach. According to [8], the node mobility can be distinguished into two types; micro and macro. The micro mobility refers to movement inside a single network domain while the macro mobility corresponds to the node movement between different network domains. Accordingly, since we are mainly dealing with a micro mobility scenario, then at this stage it's better to omit the IPv6 approach in order to minimize the incurred overhead of the utilized scheme like MIPv6 [9] (as it is considered a complicated protocol for low power devices [10]) and eliminating its burden on the nodes. The second tactic is relying on 6LoWPAN, but unfortunately this adaptation layer diverts the mobility issue to the responsibility of the routing protocols [11]. Alternatively, the remaining solution focuses

Yaarob Al-Nidawi, Harith Yahya and A. H Kemp are with the Electronic and Electrical Engineering Department, University of Leeds, LS29JT, UK, (e-mails: [elymna@leeds.ac.uk](mailto:elymna@leeds.ac.uk); [elhdy@leeds.ac.uk](mailto:elhdy@leeds.ac.uk); [A.H.Kemp@leeds.ac.uk](mailto:A.H.Kemp@leeds.ac.uk)).

<sup>1</sup> According to the IEEE 802.15.4e assumption, the coordinator must be able to collect readings of 20 LLDN devices within 10ms.

on the IEEE 802.15.4e standard and specifically the LLDN mode itself. Accordingly, the objective of this paper is to study the impact of mobility on the LLDN mode via presenting a Markov chain model that addresses the possible states a mobile node might encounter through the association process. In addition, we are introducing a mobility-aware (MA) LLDN scheme that considers the nodes mobility problem and minimizes both latency and energy consumption while maintaining the possible assumptions that the LLDN has stated. Furthermore, the proposed MA-LLDN supports multihop topology to extend the coverage of the coordinator while omitting the need for deploying further coordinators in the network. In turn, this minimizes the deployment cost and the probability of beacon collision between adjacent coordinators. The proposed approach has low latency since it delivers the readings within the same superframe. The relay nodes also act as a proxy to the coordinator where they can passively indicate the existence of the coordinator with low overhead and less association delay.

The remainder of this paper is structured as follows. Section II provides a description of relevant related work leading to an explanation of the infrastructure of the LLDN mode in section III and then section IV analyses the mobility overhead. The novel proposed MA-LLDN which tackles the impact of node mobility, is presented in section V. Analysis and discussion of our results are presented in section VI before conclusions being drawn in the final section.

## II. RELATED WORK

In a static network, the sink mobility (which can be considered here as the coordinator mobility) is said to be a solution to enhance network performance. Accordingly, to minimize the latency and energy consumption, a mobile sink is deployed that circulates through the network to collect readings as in [12-15]. Other literature addressed the issue of latency in sensor network but do not address the mobility nor are dedicated for the IEEE 802.15.4 standard [16-19]. Similarly, the recent contributions that concern the LLDN do not consider the mobility issue. Therefore, a significant part of the IoT paradigm, which is the IEEE 802.15.4e LLDN mode, has not been addressed before and needs to be evaluated comprehensively to optimize performance with regards to sensor node mobility.

Here the current enhancements to the default LLDN structure are introduced.

A. Berger *et al.* [20] improve data collection reliability of the default LLDN star topology by amending the structure with relay nodes. The objectives behind the relay nodes are to increase the transmission reliability via retransmitting unsuccessfully delivered packets and to extend the topology to two-hop networks. The authors indicate that the coordinator is stationary while the nodes might be mobile but did not address the issue of association since the target of the paper is realizing reliable transmission and 2-hop communication. The authors amended this work and improve its reliability in [21] through utilizing the combinatorial testing approach (CT) which is described in [22].

G. Patti *et al.* [23] introduce the multi-channel approach to reduce operational cycle times (superframe size). Maximizing the number of nodes increases the cycle time linearly, and hence the authors have divided the network into clusters (called subnetworks). Each cluster will have a different frequency channel to simultaneously operate without any interference with other clusters. Although this approach will minimize the cycle time for the individual subnetwork, but still the head coordinator operates for a full cycle related to the number of nodes in the total subnetworks that are connected to it.

L. Dariz *et al.* [24] improve LLDN performance via optimizing the LLDN superframe duration. This is achieved through turning the timeslot allocation procedure into a flexible and efficient allocation process. Instead of fixing the number of base timeslots in the uplink and downlink slots to a fixed size in the superframe, the number of base slots will be variable based on each node's requirement. In addition, the authors amended the superframe structure to accommodate more slots types as high-priority uplink and high-priority downlink slots to fulfil the requirements of some nodes with high priority data.

M. Anwar *et al.* [25] provide an analysis for different LLDN configuration parameters during network control design. The analysis takes into account different LLDN configuration parameters such as base timeslot size, superframe size, enabled security or not and payload size. The target is to provide a tradeoff between LLDN configuration parameters that will aid the LLDN network control design phase.

H. Kapil *et al.* [26] incorporate node relay placement strategy and error correction technique to minimize the number of retransmissions and hence, a reduced number of relays and better energy efficiency. The objective of the proposed approach is an adaptive retransmission technique by integrating a Reed Solomon error correction scheme with a relay placement mechanism (that is based on the rainbow ranking algorithm [27]). The advantage is less nodes and less energy consumption while high LLDN reliability is achieved.

## III. LLDN DESCRIPTION

IEEE 802.15.4e [4] has presented three modes of operation in addition to the default beacon-enabled and beacon-less modes. These modes are the timeslotted channel hopping (TSCH), low-latency deterministic networks (LLDN) and deterministic and synchronous multi-channel extension mode (DSME), each targeting specific types of applications and constrains. One of the important modes that gained an interest inside the research community is the LLDN mode. The LLDN mode is considered as a preferable solution among the industrial applications due to its low latency advantage. LLDN achieved LL utility through employing two strategies; (i) assigning what is called the slot owner timeslot that is dedicated for each node inside the personal operating space (POS) of a coordinator, (ii) via reducing the data frame MAC header to a single byte for data frames (excluding two FCS bytes). This is achieved by omitting the address fields and

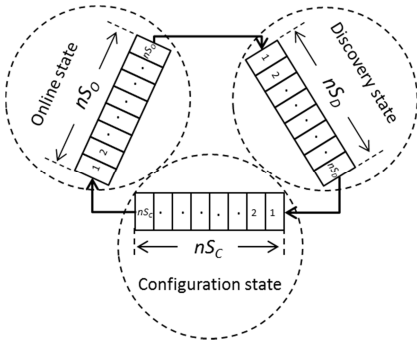


Fig. 1. Transmission states in LLDN

relying on the timeslot ( $TS$ ) index inside the superframe to determine the sender node identity. Hence, this eliminates CSMA-CA delay (caused by the contention process during each  $TS$ ) and reduces transmitting/receiving time delay.

The LLDN mode has three distinct transmission states and each has predefined superframe structure and purpose. The first transmission state is the discovery state that is initiated either during the network setup or to handle new node association to the network. The second phase is the configuration state, by which the nodes that managed to communicate with the coordinator during the discovery state shall receive network configurations during this state. The last state is the online, where the nodes can transmit their readings to the coordinator within the assigned timeslots during the configuration state. The coordinator specifies the state of transmission through the periodically transmitted beacons. Each one of the discovery, configuration and online states has a defined number of superframes during its period that will be defined by the network administrator;  $nS_D$ ,  $nS_C$  and  $nS_O$  respectively as in Fig. 1.

The discovery and configuration states share the same superframe structure but with different network purposes. The discovery and configuration superframes contain only one beacon slot and two management  $TS$ s (uplink and downlink). Although the online superframe has beacon, management, uplink and bidirectional slots, the default setting has omitted both management and bidirectional slots (as  $macLLDNmgmtTS$  is set to FALSE and  $macLLDNnumBidirectionalTS$  is set to zero). Beacons are broadcast periodically and used to synchronize the nodes, identify the present transmission state and contain an acknowledgment bitmap of the previous superframe received readings. The uplink management  $TS$  is utilized by dissociated nodes during discovery and configuration transmission states to transmit discovery response frame and configuration status frame respectively. During the downlink management slot, the coordinator shall respond to nodes' requests by either replying ACK messages (within discovery state) or configuration request frame (within configuration state).

Uplink timeslots are unidirectional (from nodes to coordinator) and the default number of  $TS$ s in the uplink is set to 20 (based on the  $macLLDNnumUplinkTS$  value) and its maximum value is 255. Transmission failure can be refreshed by permitting the nodes to retransmit within the next superframe and defined by the  $macLLDNnumRetransmitTS$ ,

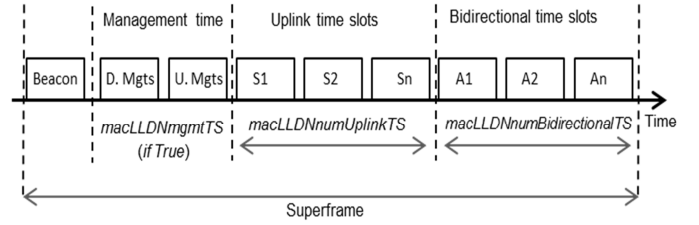


Fig. 2. General LLDN superframe structure

which specifies the number of retransmission timeslots within uplink section. The bidirectional section has  $macLLDNnumBidirectionalTS$  timeslots and the direction of transmission is indicated within the beacon fields. Fig. 2 indicates the basic layout of a general LLDN superframe structure.

Nodes seeking to join the network must follow a sequence of association steps determined by the transmission state of the upcoming superframes. Each node wishing to associate with the network must scan for beacons to determine both the existence of a coordinator and the transmission state of the current superframe. Once it has received a valid beacon that indicates a discovery state, the node sends a discovery response frame to indicate its willingness to join the intended coordinator as indicated in Fig. 3.

A node can transmit its request only during the uplink management slot (its time is defined through the beacon). The management  $TS$ s are treated as shared group  $TS$ s and the nodes commence transmission based on a simplified CSMA-CA. If the coordinator receives the request correctly, it will reply with an ACK message during the downlink  $TS$  of the next superframe. Each coordinator waits for  $macLLDNdiscoveryModeTimeout$  seconds until changing to the configuration state if no discovery response frames are received. The association process will transfer to the second phase if the coordinator indicates the configuration transmission state through the announced beacon. Once a node indicates this state, it sends a configuration status frame (during the uplink management  $TS$ ) to request network configuration parameters. The correspondent coordinator will reply with a configuration request frame that contains the assigned timeslot, its duration, transmission channel and any related information based on the network settings. Finally, the node receiving the configuration request frame replies with an ACK message to confirm successful configuration.

Studying the infrastructure of the LLDN can conclude several issues that rose by the association process and are escalated with the presence of mobile nodes. These drawbacks can degrade the network performance and violate the objectives that the LLDN is based on to support LL application limitations. We can summarize these issues into the following:

- There is no mechanism to change from transmission state to another after the network initialization phase.
- During the online state (which is the dominant state through the network lifetime) any node seeking to join the network has no feasible procedure to communicate with a coordinator, especially with the

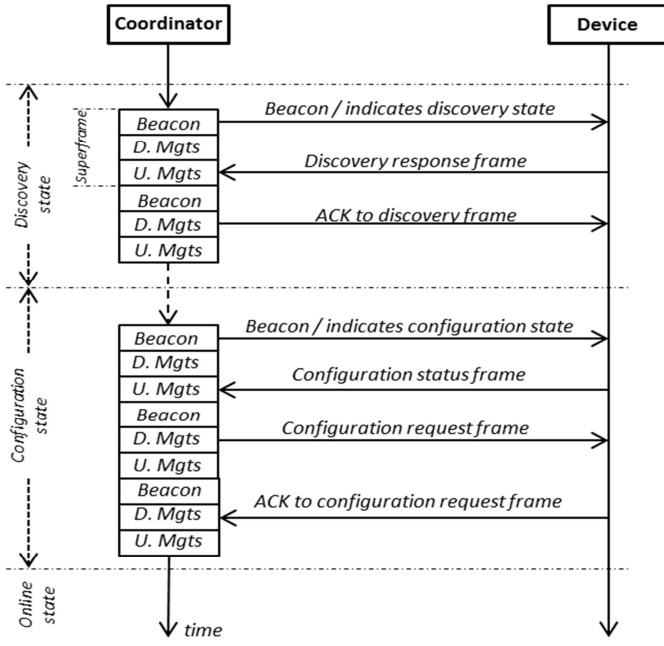


Fig. 3. Association procedure in LLDN

*macLLDNmgmTS* is set to FALSE during online state.

-The size of the management *TS* and the contention mechanism must be reconfigured to accommodate multiple orphan nodes (or mobile nodes seeking to join the network) and minimize the dissociation time to reduce latency.

- In order to commence the association process, the network must transit to the discovery state and drop the online state. This means preventing the connected nodes from transmitting regular readings and wait till completion of both discovery and configuration states. This increases latency and violates the objectivity of LLDN which can get worse in the case of high mobility, where the network has several transitions from the online state to other states.
- The LLDN is based on a simplified CSMA-CA where the *macMaxCSMABackoffs* value has been set to zero. This complicates the association process due to the announcement of a channel access failure after only a single unsuccessful CCA scan. Hence, the node has to scan for another beacon and superframe, which will maximize the dissociation interval.
- The default assumption of the LDN is based on a star topology that considers single-hop scenarios, whereas in reality and for multiple application types a multihop infrastructure is required. Considering a single hop infrastructure for highly dense network, with mobile nodes and short range transmission can cause a flaw in the design phase. First, due to the increased required numbers of coordinators in order to assure single hop transmission, this will in turn increase deployment cost and complexity. Second, this will maximize the number of dissociations due to short range transmissions and high number of mobile

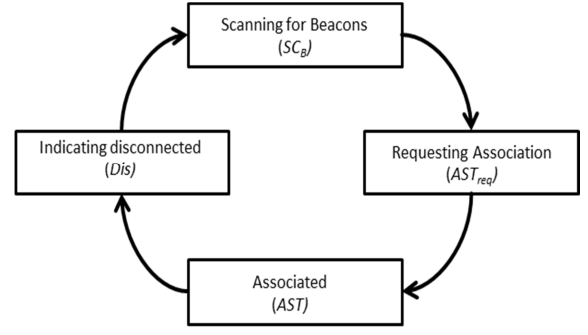


Fig. 4. Mobile node lifecycle

nodes. This maximizes the latency and degrades network availability.

#### IV. MOBILITY OVERHEAD OVER IEEE 802.15.4E LLDN

The impact of node movement and the overhead upon the network performance need to consider the lifecycle of a mobile node. The possible life stages that a mobile node encounters since deployment can be categorized into four basic steps as explained in Fig. 4. Based on this classification, we can estimate the elapsed time in each state. From this point, we have to define the possible time duration of each superframe type in LLDN, as for each transmission state there will be a different superframe duration. Discovery and configuration superframe intervals are closely related where the discovery superframe interval ( $S_D$ ) can be defined as:

$$S_D = \frac{(B_p + (T_{sz} \times 2) + (3 \times SIFS) + P_A)}{R_s} \quad (1)$$

$B_p$  is the beacon period in symbols and corresponds to physical header plus MAC header lengths (in bytes) and is multiplied by the number of symbols per byte (for the 2.4 GHz band both physical and MAC are 2).  $T_{sz}$  is the real slot size (excluding interframe spacing) of a slot and the *SIFS* corresponds to *macMinSIFSPeriod* while  $R_s$  is the symbol rate.  $P_A$  is the interval time between each beacon announcement, since the network administrator may extend the period between each superframe (in our calculation  $P_A$  is set to zero) to utilize energy (where  $P_A$  is the inactive period). The  $B_p$  can be estimated to be  $(6+7) \times 2$  symbols and  $T_{sz}$  is equal to  $(6+4+14) \times 2$  symbols, where the maximum payload (in the discovery stage messages) is 14 bytes. In addition, configuration superframe duration ( $S_C$ ) can be estimated as:

$$S_C = \frac{(B_p + (T_{sz} \times 2) + (2 \times SIFS) + LIFS + P_A)}{R_s} \quad (2)$$

Where  $T_{sz}$  here is equal to  $(6+4+14+ \text{additional\_payload}) \times 2$  and *LIFS* corresponds to *macMinLIFSPeriod*. *additional\_payload* depends on the application and could be the frequency channel, assigned timeslot etc.

Finally, online superframe ( $S_O$ ) can be estimated as indicated in [4] while identifying the MAC payload size:

$$S_O = \frac{(B_p + SIFS + (N_{TS} \times T_{sz}) + (N_{TS} \times LIFS) + P_A)}{R_s} \quad (3)$$

Where  $N_{TS}$  represents the possible number of timeslots in the

TABLE I  
SYMBOLS AND DEFINITIONS

Symbol / Abbreviation	Definition
$AST_{req}$	Requesting association
$AST$	Associated to the network
$Ad_i$	represents $i^{th}$ adjacent POS
$B_p$	Beacon period
$BE$	Backoff exponent
$CW$	Contention window length
$Dis$	Indicating dissociated
$D_m$	Density metric
$D$	Distance
$D\_Mgts$	Downlink management timeslot
$E_{thr}$	effective throughput
$h$	Hop index
$i\_Mgts$	Image of a management timeslot
$K$	Possible number of movements inside a POS
$L_h$	latency in a given hop
$L_D$	Expected latency during discovery state
$L_C$	Expected latency during configuration state
$L_{CA}$	Expected latency during acknowledging configuration state
$LOS_D$	number of lost data frames
$M_m$	Mobility metric
$Mgts$	Management timeslots
$N_m$	number of mobile nodes seek to associate the coordinator
$N_{ert}$	set of existed nodes in a POS
$N_A$	set of active nodes
$N_a(i)$	number of nodes get associated at a given time $t_i$
$N_w$	Number of nodes waiting to associate
$nS_o$	the number of online superframes
$nS_D$	the number of discovery superframes
$nS_C$	the number of configuration superframes
$nP_h$	number of mobile nodes attached to a given proxy
$O_c$	preferred number of online superframes
$P_A$	Interval time between two beacons
$P_{th}$	Maximum number of online superframes
$R$	Transmission range
$Req_s$	Maximum configuration request size
$R_s$	Symbol rate
$R_t$	Total running time
$S$	Superframe in general (any superframe type)
$S_D$	discovery superframe interval
$S_C$	configuration superframe interval
$S_O$	online superframe interval
$SC_B$	Scanning for beacon phase
$S_{Bmgs}$	Size of a single slot in Mgts
$TS$	Timeslot index
$T_{SZ}$	Timeslot size (excluding interframing space)
$T_{ack}$	Turnaround time
$T_{Mgts}$	Time counter after what the proxy node accepts association request
$t_s$	Settle time in a POS
$U\_Mgts$	Uplink management timeslot
$V_x(t)$	velocity of node $x$ at time $t$
$x_D$	number of mobile nodes successfully transmitted discovery response frame
$\gamma_D$	Probability of the first CCA returns free (during discovery state)
$\alpha$	Probability of receiving a beacon
$\beta$	probability of a received beacon determines discovery state
$\delta_D$	Probability of the second CCA returns free (during discovery state)
$\theta_t$	Probability to complete association within $t_s$

uplink unidirectional field and can be either set to  $macLLDNumUplinkTS$  value or can be varied based on the number of nodes in a POS. Here  $T_{SZ}$  is the actual slot size of a single base timeslot (excluding interframe spacing) in the uplink and equal to  $(6 + 3 + \text{payload\_size}) \times 2$ . Table I

TABLE II  
IEEE 802.15.4E MAC ATTRIBUTES

Attribute	Definition
$macLLDNumMgmtTS$	Indicate the existence of management timeslots (Boolean value)
$macLLDNumBidirectionalTS$	Number of bidirectional timeslots
$macLLDNumUplinkTS$	Number of uplink timeslots
$macLLDNumRetransmitTS$	Number of retransmission timeslots
$macLLDDiscoveryModeTimeout$	Time threshold to change from discovery to configuration state
$macMaxCSMABa-ckoffs$	Maximum number of backoffs the CSMA can attempt
$SIFS$	Short interframe space
$macMinSIFSPeriod$	Defined value of $SIFS$ in the standard
$LIFS$	Long interframe space
$macMinLIFSPeriod$	Defined value of $LIFS$ in the standard
$aMaxLostBeacons$	The maximum value of missed beacons to announce the node is orphan
$aTurnaroundTime$	Required time for a device to change from transmit to receive state and vice versa

presents a list of symbols and their definitions used in this paper, while Table II illustrates the utilized MAC attributes.

As in Fig. 4, there are four states that a mobile node may encounter, scanning for beacon interval ( $SC_B$ ), requesting association ( $AST_{req}$ ), fully Associated to network ( $AST$ ) and indicating disconnect ( $Dis$ ) (or orphan).

The first phase of this lifecycle that will be estimated is  $Dis$ , where it can have two values based on the methodology followed to indicate the dissociation (announce the node is orphan), which is either based on the number of lost beacons or missed ACK messages.

$$Dis = \begin{cases} aMaxLostBeacons \times S_o \\ nmACK \times S_o \end{cases} \quad (4)$$

$nmACK$  represents the number of missed ACK messages. Regarding the second phase, scanning for beacon interval ( $SC_B$ ) can be expressed as:

$$SC_B \cong \begin{cases} \frac{S_D}{2} & (5) \\ \left( \frac{S_O}{2} \right) + \left( \sum_{j=1}^{\lfloor \frac{O_c}{(M_m + D_m)/2} \rfloor} S_{Dj} \right) \bmod P_{th} & (6) \\ \frac{(t_2 - t_1)^2}{T} + \frac{((T - t_1) - t_2)^2}{T} & (7) \\ \frac{S_o + (nS_o \times S_o) + (nS_C \times S_C)}{2} & (8) \end{cases}$$

In these four scenarios, (5) is the case where the coordinator is in the discovery transmission state. Here we are assuming perfectly scheduled timeslots, but in the case of different superframes durations, it will follow the random incidence paradox [28, 29] and expressed as:

$$\frac{\sigma^2 \mathbb{E}[S]^2}{2 \mathbb{E}[S]} \quad (9)$$

But since we are dealing with tightly synchronized nodes,

perfectly scheduled and fixed superframes duration are assumed, so  $SC_B = (S/2)$ , where  $S$  is any superframe ( $S_D$ ,  $S_C$  or  $S_O$ ). In the case of the coordinator in the online state, the scanning and waiting time is dependent on the interval that is adjusted to transfer from the online to discovery state as in (6). The approximated scenario is to harness both the mobility metric ( $M_m$ ) and density ( $D_m$ ), which can be derived both based on [30, 31] and [32] respectively, to determine the duration between each transfer.  $O_c$  represents the preferred number of online superframes in each period before flipping to a discovery state while  $P_{th}$  is the maximum number of online superframes after which there must be a discovery state. Based on these parameters it will be easy to efficiently provide a tradeoff between latency and dissociation time, increasing mobility and density metric will increase the number of discovery superframes per online superframes in order to accommodate more mobile nodes and reduce the scanning waiting time. According to [31], the mobility metric can be considered as the average relative speed of nodes over the possible number of node pairs and running time. Hence, for a given graph  $G = (N, P)$ , where  $N$  is a set of sensor nodes and  $P$  is a set of links between the nodes and  $\in N$ , the mobility metric  $M_m$  can be expressed as [30, 31]:

$$M_m = \frac{1}{|P|} \sum_{x_1=1}^{|N|} \sum_{x_2=1}^{|N|} \frac{1}{R_t} \int_0^{R_t} |V_{x1}(t) - V_{x2}(t)| dt \quad (10)$$

Where  $R_t$  is the total running time,  $V_x(t)$  is velocity of node  $x$  at time  $t$ . In addition, according to [32] the density metric  $D_m$  can be expressed as:

$$D_m = \frac{|N| \pi R^2}{A} \quad (11)$$

Here  $A$  is the scattered area and  $R$  is the transmission range. Returning to (7), which holds the condition that two coordinators exist, for a given period of time  $T$ . If the first coordinator announces at  $t_1$  and the second announces at  $t_2$  and  $t_1, t_2 \in T$ , then we have two inter-arrival times,  $(t_2 - t_1)$  and  $((T - t_1) - t_1)$ . Thus, the expected waiting time can be expressed as in (7).

The fourth scenario, as in (8), is applied when there is a defined structure of the network transmission states. The scanning time in this condition is based on the number of online superframes ( $nS_O$ ) and the number of configuration superframes ( $nS_C$ ) that are both defined prior to network deployment.

The third phase of the mobile node lifecycle is the  $AST_{req}$ , which will be completely dependent on the ratio of the number of both discovery and configuration superframes to the online superframes. In addition, it will follow the impact of the number of mobile nodes entering the same POS at the same time besides the nodes speed and transmission range. Hence, Fig. 5 presents a Markov chain that models the possible states for a mobile node during the association process. A mobile node's condition can be described in three stochastic processes; node status, backoff condition and CCA outcome ( $s(t)$ ,  $b(t)$  and  $c(t)$  respectively). The possible states of  $s$  are orphan, received beacon, discovering, configuring,

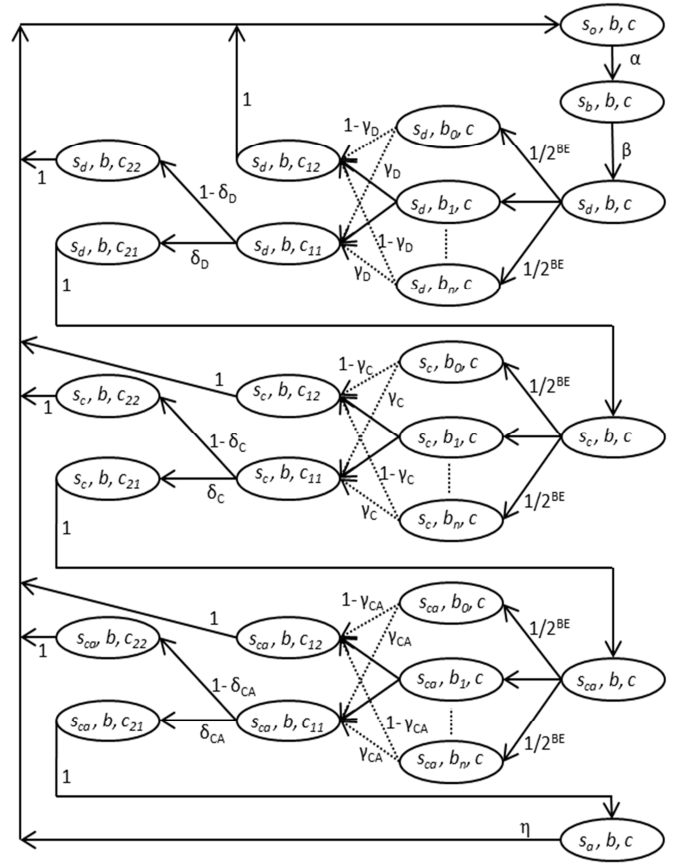


Fig. 5. Markov chain for mobile node transitions in LLDN

configuring\_ACKing and associated, which will be presented as  $s = \{s_O, s_D, s_C, s_{CA}, s_A\}$ . Meanwhile,  $b$  will be varied in the range  $[0, 2^{BE} - 1]$  and presented as  $b = \{b_0, b_1, \dots, b_n\}$ . The backoff exponent,  $BE$ , will be set to  $macMinBE$  value. Finally,  $c$  represents the possible states of the two CCA processes as  $CCA_{1\_free}$ ,  $CCA_{1\_busy}$ ,  $CCA_{2\_free}$  and  $CCA_{2\_busy}$  and presented as  $c = \{c_{11}, c_{12}, c_{21}, c_{22}\}$ . The probability ( $\alpha$ ) of receiving a valid beacon depends on the amount of coverage percentage within the scattered area (there is an adequate number of coordinators to cover the whole area of deployment). In this paper, we will always assume that we have a well scattered deployment,  $\alpha = 1$ . The probability ( $\beta$ ) of the received beacon in determining a discovery state will base on the adjusted ratio of discovery state to other transmission states. During the network initialization period,  $\beta = 1$  for at least a period of  $macLLDNdiscoveryModeTimeout$  if no node requests association. Meanwhile, within the network steady state period,  $\beta$  can be expressed as:

$$\beta = \frac{macLLDNdiscoveryModeTimeout}{\left( \sum_{j=1}^{\lfloor \frac{O_c}{(M_m + D_m)/2} \rfloor} S_{Dj} \right) \bmod P_{th} + (S_C \times x_D)} \quad (12)$$

Where,  $x_D$  is the number of mobile nodes that have successfully transmitted discovery response frames and received ACK messages. The probabilities of the first CCA and second CCA (during discovery state) ( $\gamma_D$ ,  $\delta_D$ ) returning a free channel within a given  $BE$  value ( $b_i$ ) are expressed in (13) and (14) respectively.

$$\gamma_{D(bi)} = \frac{(2^{BE} - 1) - b_i}{(2^{BE} - 1)} \frac{1}{N_m} \quad (13)$$

$$\delta_D = \frac{1}{\sum_{b_i} N_m \gamma_{D(bi)}} \quad (14)$$

Where  $N_m$  corresponds to the number of mobile nodes seeking to associate with the coordinator within the same superframe and can be derived as:

$$N_m = \mathbb{E}[|N_{crt}| - |N_A|] + \sum_j Ad_j + |N_w| \quad (15)$$

$N_{crt}$  is a set of existed nodes in the POS and  $N_A$  is a set of active nodes, where  $N_A \in N_{crt}$ .  $Ad_i$  represents  $i^{\text{th}}$  adjacent POS and  $j$  is the total number of adjacent POSs,  $N_w$  is a set of nodes already in the POS and waiting for the discovery state.

Moreover, during the configuration state, the probabilities of the first CCA and second CCA ( $\gamma_C$ ,  $\delta_C$ ) returning a free channel are expressed in (16) and (17) respectively.

$$\gamma_{C(bi)} = \frac{(2^{BE} - 1) - b_i}{(2^{BE} - 1)} \frac{1}{X_D \times nS_D} \quad (16)$$

$$\delta_C = \frac{1}{\sum_{b_i} (X_D nS_C) \gamma_{C(bi)}} \quad (17)$$

$X_D$  denotes the number of nodes managed to receive ACK for the discovery response frame. Finally, the probabilities of the first and second CCA ( $\gamma_{CA}$ ,  $\delta_{CA}$ ) returning a free channel in the acknowledgement phase of the configuration state are as follow:

$$\gamma_{CA(bi)} = \frac{(2^{BE} - 1) - b_i}{(2^{BE} - 1)} \frac{1}{X_C \times nS_C} \quad (18)$$

$$\delta_{CA} = \frac{1}{\sum_{b_i} (X_C nS_C) \gamma_{CA(bi)}} \quad (19)$$

$X_C$  denotes the number of nodes which managed to receive a configuration request frame.

Accordingly, we can calculate the relevant probabilities of each transmission mode to conclude the probability of associating to a coordinator. The probability of receiving an ACK message during the discovery state is:

$$p(s_{cr}, b, c | s_o, b, c) = \alpha \beta \delta_D \sum_{2^{BE}} \frac{1}{2^{BE}} \gamma_D \quad (20)$$

And the probability of receiving the required synchronization information during the configuration state is:

$$p(s_{ca}, b, c | s_{cr}, b, c) = p(s_{cr}, b, c | s_o, b, c) \delta_C \sum_{2^{BE}} \frac{1}{2^{BE}} \gamma_D \quad (21)$$

Finally, the probability of associating to the coordinator is:

$$p(s_a, b, c | s_{ca}, b, c) = p(s_{ca}, b, c | s_{cr}, b, c) \delta_{CA} \sum_{2^{BE}} \frac{1}{2^{BE}} \gamma_{CA} \quad (22)$$

The latency during either discovery or configuration state is determinant on the number of mobile nodes, since (as in the

standard) we assume that the coordinator shall stay at each state until responding to all requested nodes within POS. Therefore,  $AST_{req}$  can be derived based on the incurred expected latency at each state. The expected latencies ( $L_D$ ), ( $L_C$ ), ( $L_{CA}$ ) during the discovery, configuration and acknowledging configuration states respectively can be estimated as:

$$\mathbb{E}(L_D) = \sum_{j=1}^{nS_D} (1 - p(s_{cr}, b, c | s_o, b, c))^{j-1} p(s_{cr}, b, c | s_o, b, c) (S_D \times j) \quad (23)$$

$$\mathbb{E}(L_C) = \sum_{j=1}^{nS_C} (1 - p(s_{ca}, b, c | s_{cr}, b, c))^{j-1} p(s_{ca}, b, c | s_{cr}, b, c) (S_C \times j) \quad (24)$$

$$\mathbb{E}(L_{CA}) = \sum_{j=1}^{nS_C} (1 - p(s_a, b, c | s_{ca}, b, c))^{j-1} p(s_a, b, c | s_{ca}, b, c) (S_C \times j) \quad (25)$$

Hence, the expected waiting time during the association request phase  $AST_{req}$  is:

$$AST_{req} = L_D + L_C + L_{CA} \quad (26)$$

On a second hand, in order to determine a successful association, the required time to associate must be less than a settle time ( $ts$ ) in a POS. Thus, the probability ( $\theta$ ) to complete association is:

$$\theta_t = 1 - \frac{Dis + SC_B + AST_{req}}{ts} \quad (27)$$

The  $ts$  parameter is dependent on several elements as node speed, possible trajectories inside a POS and coordinator coverage. Therefore, for a mobile node under the random waypoint mobility scenario, there will be three basic elements; node speed, possible moving distance and pause time. For a node speed  $sp$  in the range  $[sp_l, sp_n]$ , distance  $D$  in the range  $[d_l, d_n]$  and pause time  $p$  in the range  $[p_l, p_n]$ , the expected settle time can be defined as:

$$ts = \frac{\sum_{i=1}^k \mathbb{E}[d]_i}{\mathbb{E}[sp]} + \sum_{i=1}^k \mathbb{E}[p]_i$$

$$= \frac{\sum_{i=1}^k \left( \int_{d_1}^{d_n} D \frac{1}{d_n - d_1} dD \right)_i}{\int_{sp_1}^{sp_n} sp \frac{1}{sp_n - sp_1} dsp} + \sum_{i=1}^k \left( \int_{p_1}^{p_n} p \frac{1}{p_n - p_1} \right)_i$$

Hence, settle time is:

$$ts = \frac{\sum_{i=1}^k \left( \frac{d_n + d_1}{2} \right)_i}{\frac{sp_n + sp_1}{2}} + \sum_{i=1}^k \left( \frac{p_n + p_1}{2} \right)_i \quad (28)$$

Where  $k$  is the possible number of movements (or the possible epochs before leaving POS) and is affected by the transmission range of the coordinator and  $D$ . In this work we

are not interested in investigating the stochastic features of the random waypoint mobility model while a comprehensive analysis can be found in [33, 34].

The probability of leaving the POS ( $\eta$ ) will be dependent on the transmission range ( $R$ ) of the sensor nodes and the total number of movements inside a given POS (assuming a straight line trajectory in a POS), expressed in (29).

$$\eta = \frac{1}{2 R_{dBm}} \sum_{i=1}^k \mathbb{E}[d]_i \quad (29)$$

For a better network performance in a mobile sensor network environment, a dissociation function must be introduced, which is a measure of the number of nodes that are dissociated. Thus, the target of a mobile sensor network must always seek for low dissociation function to gain high network connectivity and availability. This measure can be derived based on the Kaplan-Meier estimator [35]. Thus, for  $n$  distinct event times  $t_1 < t_2 < \dots < t_n$ , the dissociation function ( $\hat{S}(t)$ ) for a total time  $t$ , that  $t_1, t_2, \dots, t_n \in t$ , can be expressed as in (30). Where,  $N_a(i)$  represents the number of nodes get associated at a given time  $t_i$ .

$$\hat{S}(t) = \prod_{i=1}^n \left[ 1 - \frac{N_{m(i)} - N_{a(i)}}{N_{m(i)}} \right] \quad (30)$$

One of the issues that need to be highlighted is the node throughput that is crucial for several sensor network applications, especially that requires streaming [36, 37]. The throughput of LLDN network is related to the amount of time that the coordinator is within the online state. Therefore, we have to estimate the number of lost data frames ( $Los_D$ ) after each transfer from the online to other states, which can be expressed as:

$$Los_D = \left\lfloor \frac{nS_D \times S_D + nS_C \times S_C}{S_O} \right\rfloor \quad (31)$$

In the meantime, the effective throughput ( $E_{thr}$ ) in (bps) of the network can be defined as:

$$E_{thr} = \left( \frac{MSDU \times 8}{S_o} \right) \left( 1 - \frac{nS_D \times S_D + nS_C \times S_C}{nS_o \times S_o} \right) \quad (32)$$

Where  $nS_o$  is the number of online superframes and the data payload (MAC service data unit, MSDU) is the actual payload data size in octets as defined by the standard.

Furthermore, the packet delivery ratio (PDR), which is related to the impact of dissociation, during a given  $ts$  time can be expressed as:

$$PDR_{association} = \frac{ts - (Dis + SC_B + AST_{req})}{ts} \quad (33)$$

The impact of transferring each time from the online state can lead to PDR degradation and can be calculated as:

$$PDR_{transfer} = 1 - \frac{Los_D}{nS_o} \quad (34)$$

## V. PROPOSED ENHANCED AND MOBILE-AWARE LLDN SCHEME

From the previous sections, we can conclude two main requirements to achieve better network performance, which are low latency and multihop infrastructure. Since the LLDN is designated for a star topology, then there must be a mechanism to facilitate the multihop feature which supports both node mobility and LL. Comparing the star topology to other different topologies for the case of IEEE 802.15.4 infrastructure, it has less latency but unfortunately has less success probability [38]. Conversely, if we are looking for low dissociations, then the network has to be assisted with multiple coordinators to guarantee low waiting time prior to achieve association. This led us to the strategy of increasing the number of coordinators, but this will unfortunately open the gate to another issue, which is the overlapped beacons collision. Beacons of adjacent coordinators collide due to overlapped communication range and this issue has been addressed in several work [39-41]. Therefore, the objective of the proposed approach here is:

- To minimize the dissociation time and increase the mobile node connectivity.
- Determining how the latency and collision can be minimized.
- To support a multihop paradigm while omitting extra coordinators.
- Combining the advantages of both tree and star topologies?

A comprehensive analysis in [38] shows that the tree topology outperforms the star topology in terms of transmission success probability, but the problem with a tree strategy is significant latency. Thus, we have to figure out an approach that provides multihop (tree infrastructure) while minimizing the encountered delay. One of the approaches that could be utilized is clustering [42, 43], this technique is suitable to minimize the impact of collisions and maximizes transmission success rate but in turn increases the latency in the tree infrastructure. Hence our problem must be tackled through modifying the existed LLDN superframe infrastructure. Accordingly, the proposed approach is based on two principles; first, defining the concept of proxy coordinator and the notion of passive beacon and second, modifying the LLDN superframe.

The concept of passive beacons can be realized by forcing each node to add an extra two bytes to the MAC header of data frames, one byte preamble (*preamble\_1*) and one byte for the time that the proxy node can receive an association request. The nodes need not to include the extra two bytes in each data frame, but this can be performed in every interval of time and this interval is influenced by the mobility metric. This concept has been called the passive beacon since the nodes are not beaconing but are indicating passively (through data frames) the minimum relevant information regarding node association and thus, the data frames are acting as beacons. Therefore, the nodes are acting as a proxy to the original coordinator within the LLDN network. Any node that acts as a coordinator will be denoted as a proxy.

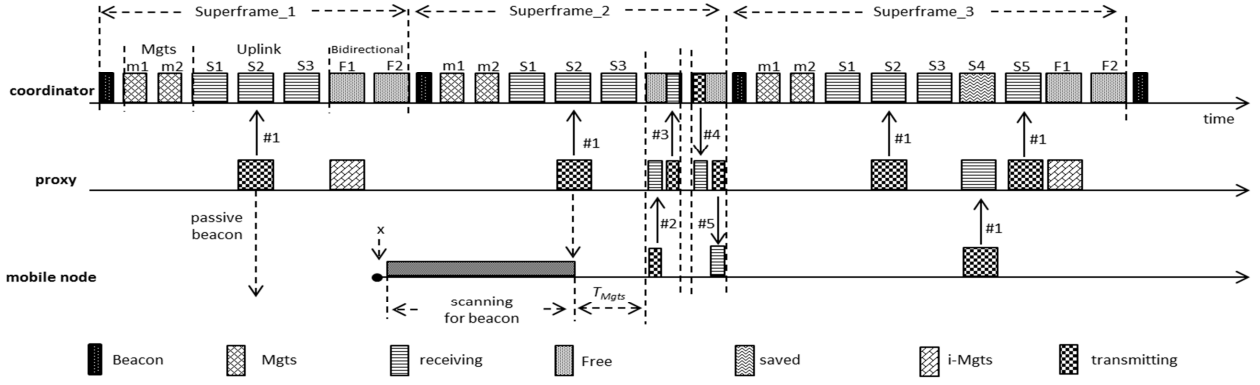


Fig. 6. 2-hops mobile node association in MA-LLDN

A mobile node that can't detect any beacons, can listen for existing data frames and scan the header for the preamble byte. If *preamble\_1* exists, then the next byte is the time ( $T_{Mgts}$ ) by which the proxy node is accepting association requests (see Fig. 6).  $T_{Mgts}$  is the time interval between the transmitted data frame and the time a proxy switches the radio on to receive a request. In order to mitigate any chance of collision with the coordinator, the proxy utilizes the F slots (additional free slots the coordinator allocates for the purpose of permitting proxy node to accept association requests freely). Each proxy adjusts the time to accept association requests within defined slot boundaries (called image timeslot (*i-Mgts*)) that coincide with the first bidirectional (F1) slot in the superframe. The duty of the coordinator in this case is to ensure that there are always at least two free F timeslots in the bidirectional field of the superframe to be used by the proxy nodes. This will ensure that the management timeslots *i-Mgts* (of proxies) are not overlapping with the current utilized (transmitting data) slots in the superframe. The bidirectional slots will always be used as the first  $n/2$  slots as uplink and the second  $n/2$  slots as downlink, for slots [F1-Fn], where  $n$  here is the number of slots in the bidirectional field.

Once a proxy receives an association request (message #2 in Fig. 6) during the *i-Mgts*, it will relay the request to the coordinator within the same slot (message #3), since this slot has been freed within the superframe for the purpose of this task. During the next timeslot, the coordinator responds with the required information (message #4) in order to synchronize the mobile node (allocated timeslot, transmission channel, etc.). The proxy has to relay the information back to the mobile node (message #5) and finalize the association process. Hence, the entire process is accomplished within only two consecutive timeslots (in the case of two hops).

The coordinator upon the addition of a new mobile node, adds four additional timeslots to the uplink and bidirectional fields for each upcoming superframe. That will be one for transferring data from mobile node to proxy (slot S4), one for transferring data from proxy to coordinator (slot S5) and two (slots F1 and F2) for the purpose of *i-Mgts* slots. The *i-Mgts* slots are harnessed by the proxy nodes to permit more mobile nodes in the future to join the network.

The modified superframe has reduced the latency by instructing the proxies to relay the data frames of the nodes,

which are not within the first hop, within the same superframe. Hence, the latency  $L_h$  for a node in a given hop ( $h$ ) is:

$$L_{h[\min]} \leq L_h \leq L_{h[\max]}$$

$L_{h[\min]}$  and  $L_{h[\max]}$  can be calculated as:

$$L_{h[\min]} = \left[ \sum_{i=2}^h \left( \frac{i(i+1)}{2} - 1 \right) nP_i + (h-1) + L_{h-1} \right] (T_{SZ} + IFS) \quad (35)$$

$$L_{h[\max]} = \begin{cases} \left[ \left( \frac{h(h+1)}{2} - 1 \right) + \sum_{i=2}^h \left( \frac{i(i+1)}{2} - 1 \right) nP_i \right] (T_{SZ} + IFS); & \text{for } h > 1 \\ (T_{SZ} + IFS); & \text{otherwise} \end{cases} \quad (36)$$

Where the *IFS* corresponds to the interframe spacing that could be either *macMinSIFSPeriod* or *macMinLIFSPeriod*.  $nP_h$  refers to the number of mobile nodes attached to a given proxy (within the route) at hop  $h$ .

Since the maximum configuration request size ( $Req_s$ ) is 48 symbols (physical and MAC header plus configuration status payload), then the required time to commence transmission of two messages is always less than  $T_{SZ}$ . Hence, a single timeslot  $T_{SZ}$  in the uplink field of a superframe can accommodate two transmissions, sending an association request and replying with an ACK message. Thus, this property will be always true:

$$Req_s + T_{ack} + ACK_s + SIFS < T_s \quad (37)$$

$ACK_s$  is the ACK message size which can't exceed 48 symbols (physical and MAC header plus configuration request payload) and  $T_{ack}$  is the turnaround time and corresponds to a *TurnaroundTime* value, which is 12 symbols. According to the standard, the required time for a node to switch from receive to transmission mode and vice versa is equal to a *TurnaroundTime* symbols. Thus, we include it in our analysis.

Considering more than two hops is also still feasible, but the coordinator must provide at least four F slots in the bidirectional field to accomplish an association. This is caused by the  $T_{SZ}$  size limitation, where it is impossible to handle three transmissions in a single  $T_{SZ}$ . The required time is larger

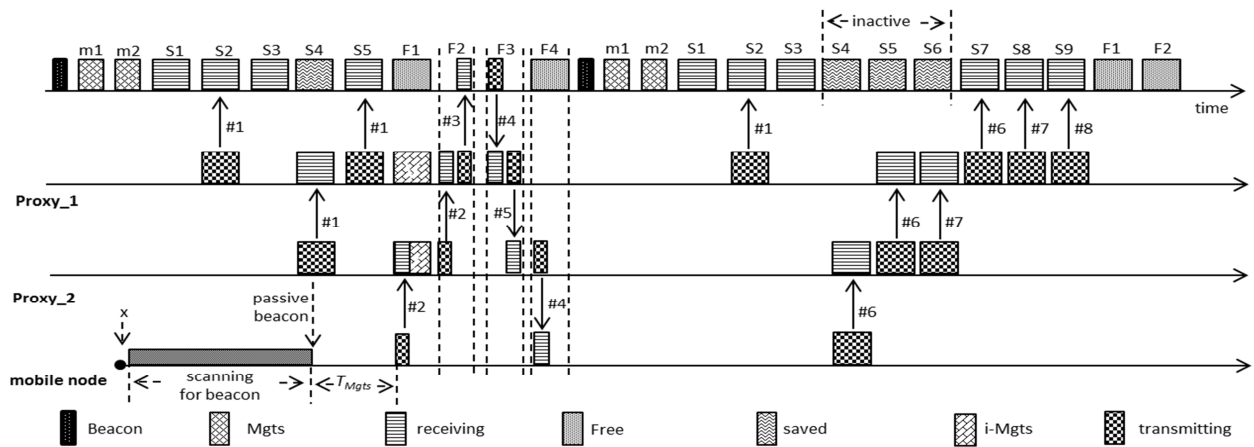


Fig. 7. 3-hops mobile node association in MA-LLDN

the size of individual  $T_{SZ}$ :

$$3 \times Req_s + 2 \times T_{ack} + 3 \times ACK_s + SIFS > T_{SZ} \quad (38)$$

Therefore, for 3-hops and 4-hops mobile nodes, the coordinator has to allocate at least four slots to complete the association process as in Fig. 7. The coordinator must be adjusted based on the number of permitted hops in the network. Hence, for a network that allows for three hops, the coordinator is forced to allocate four slots [F1-F4] in order to guarantee smooth mobile node association.

Seeking to avoid the hidden-node problem [44, 45] in multi hop networks, transmitting regular readings to the coordinator must be accompanied with the allocation of extra slots to the superframe. These slots will be called “saved” and the coordinator may stay inactive during these slots to save energy. The saved slots are required for the purpose of transferring data between mobile nodes and proxies as in {S4} in Fig. 6 and {S4, S5, S6} in Fig. 7.

For a given network, if hop  $h=2$  the set of proxy nodes

$$Prox_2 = [R_1^2 - R_n^2]$$

and at  $h=3$  the set of proxies  $Prox_3 = [R_1^3 - R_m^3]$ . Then we can describe the negotiation between a given mobile node  $M_x$ , proxy and coordinator  $C$  during the association phase at  $h=2$  and  $h=3$  as in Table III.

Regarding the case of  $h=4$ , it will still be feasible to conduct the association within four slots [F1-F4] due the property of (38).

There are two important drawbacks in the structure of the LLDN. The first one is its dependency on three transmission states and the second is the sequence of the  $Mgts$  in the superframe. The first issue is caused by the types of transmission states which influence two crucial aspects in the network, throughput and association. The throughput is affected due to the transfer from the online state to other states, which will make the nodes refrain transmitting data until the coordinator switches again to the online state. The association issue has already been indicated previously in sec. III. Accordingly, the first enhancement can be achieved through swapping the  $D\_Mgts$  with the  $U\_Mgts$ . Therefore, the coordinator can reply within the same superframe to the

TABLE III  
MULTIHOP COMMUNICATION MESSAGES

$h=2$	$h=3$
F1: $M_x \rightarrow R'_x$	F1: $M_x \rightarrow R^2_x$
F1: $R \rightarrow C$	F2: $R^2_x \rightarrow R'_x$
F2: $C \rightarrow R'_x$	F2: $R'_x \rightarrow C$
F2: $R'_x \rightarrow M_x$	F3: $C \rightarrow R'_x$
	F3: $R'_x \rightarrow R^2_x$
	F4: $R^2_x \rightarrow M_x$

Thus, during  $U\_Mgts$ , the mobile node requests association and the coordinator responds immediately at  $D\_Mgts$ . The second enhancement can be realized through modifying the structure of  $Mgts$ . These two slots must be existed in each superframe and not optional as indicated by the standard, at least the superframe includes the  $Mgts$  in every period of time that corresponds to the mobility metric. In addition, in order to preserve network throughput and to minimize the dissociation time, the structure of the transmission states must be altered. According to the LLDN, the nodes can only associate through the sequence of discovery then configuration states. These two states can be observed during the initialization phase of the network while during the steady state and since we already force the coordinators to keep  $Mgts$  in each superframe, these states can be omitted. Hence, the network keeps operating inside the online state without switching to other states and considers the  $Mgts$  to accomplish the required association process, as indicated in Fig. 6 and 7.

For limited power coordinators and multihop network, there will be some limitations regarding beaconing. This affects the period of beaconing and then maximizes the superframe duration  $S_O$ . This issue also can be caused by increasing the number of LLDN devices within the POS that in turn maximizes  $S_O$ . In this case,  $N_m$  and  $S_O$  influence the number of nodes  $N_w$  waiting to associate and this value could be increased as the coordinator increases  $S_O$ . Thus, there must be a mechanism to facilitate multiple mobile nodes associations within the same superframe. In addition, restructuring the

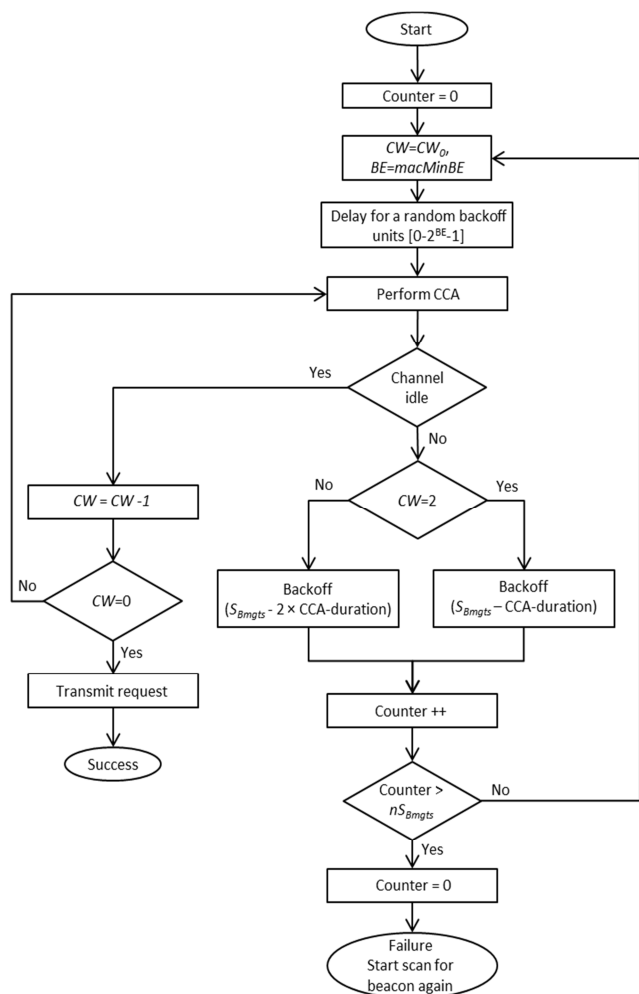


Fig. 8. Backoff mechanism in  $Mgts$  of MA-LLDN

$Mgts$  to accommodate multiple nodes and maintain these slots properly will preserve the functionality of the  $Mgts$  as dedicated by the standard which can be utilized for other purposes instead of association. Therefore, a backoff mechanism is proposed in this paper to manage mobile node access during  $Mgts$ .

The backoff technique relies on amending the  $Mgts$  size that can be achieved through utilizing the timeslot size field in the beacon. In addition, bits 5-7 in the flag fields of the beacon are utilized to define the number of base time slot in each  $Mgts$ . Hence, we can construct the  $Mgts$  as a slotted access field by which it can resemble the contention access period (CAP) in the beacon enabled mode. The size of each slot ( $S_{Bmgts}$ ) inside the  $Mgts$  can be estimated to be (in symbols):

$$S_{Bmgts} = \text{Max\_Backoff\_Time} + \text{Total\_CCA\_duration} + \text{Maximim\_transmission\_time} + \text{SIFS}$$

$$SBmgts = [(2^{BE} - 1) \times 20] + (2 \times 8) + 48 + 12$$

Hence, the maximum  $S_{Bmgts}$  size can be 216 symbols. The maximum transmission time has been set to 48 symbols with the assumption that the association request payload contains (full address, short address and 4-Byte for application-specific purposes). The proposed backoff mechanism is an amended

version of the simplified CSMA-CA and the number of contentions is limited by the number of slots in a single  $Mgts$  ( $nS_{Bmgts}$ ). Fig. 8 simplifies the proposed backoff algorithm, where  $CW$  and  $BE$  are set to 2 and 3 respectively as indicated by the standard for LLDN mode.

## VI. RESULTS AND ANALYSIS

This section highlights three important aspects that are influenced by node mobility in LLDN network. PDR in static networks can be affected primarily by the number of collisions and interference within a network, but for mobile nodes new factors are included that degrade network PDR. Moreover, in LLDN networks there are two additional factors that reduce PDR. These are the excessive dissociations (due to changing POS) and the regular transfers from online state to other states. Thus, the first part of this section presents two factors related to PDR, one concern with the overhead of dissociation (named  $PDR_{dissociation}$ , for dissociated nodes) and the second considers the impact of transferring away from the online state (named  $PDR_{transfer}$ , for nodes already connected) that prevent the node from sending readings until the end of both discovery and configuration states. The  $PDR_{transfer}$  is dependable here on seven parameters that are  $S_O$ ,  $S_C$ ,  $S_D$ ,  $nS_D$ ,  $nS_C$ ,  $nS_O$  and number of slots in the superframe (corresponds to  $macLLDNnumUplinkTS$ ). Increasing the number of slots maximizes the  $S_O$  value.  $S_C$  and  $S_D$  values are always fixed to 2.976ms and 2.528ms respectively since the structure of the superframe in these two states rarely changes (fixed number of fields in the superframe). In addition, the values of  $nS_C$  and  $nS_D$  will always be equal since there must be an equivalent number of configuration superframes to accommodate the possible number of mobile nodes that have been considered in the discovery stage. In order to tackle the node mobility and achieve better network connectivity, the network administrator must increase the number of discovery and configuration superframes,  $nS_D$  and  $nS_C$ . Accordingly, this approach will minimize network  $PDR_{transfer}$  due to the maximization of the period that the nodes are obliged to refrain transmitting readings prior to completion of discovery and configuration states. The  $S_O$  duration (influenced by the number of slots) can worsen the case for low durations as indicated in Fig. 9 to Fig. 12, which show a varying number of slots. The important feedback here is determining the ratio of discovery and configuration to online superframes ( $(nS_C + nS_D)/nS_O$ ). Accordingly, to achieve a PDR no less than 98%, for slots ( $macLLDNnumUplinkTS$ ) = 1, 8, 20 and 40, then the ratio of the number of discovery and configuration to online superframes must be no larger than 0.08, 0.2, 0.33 and 1 respectively ( $nS_C$  &  $nS_D$  fixed to 50). Here the ratio corresponds to the number of online superframe to one discovery and one configuration superframe.

The second parameter is  $PDR_{dissociation}$  which is affected by the number and interval of dissociations periods from the network. The  $PDR_{dissociation}$  is basically dependent on the transmission range and node mobility metric. Fig. 13 shows the impact of increasing the transmission range from 50m to 150m on the PDR. In this scenario, the impact of the  $nS_O$  has

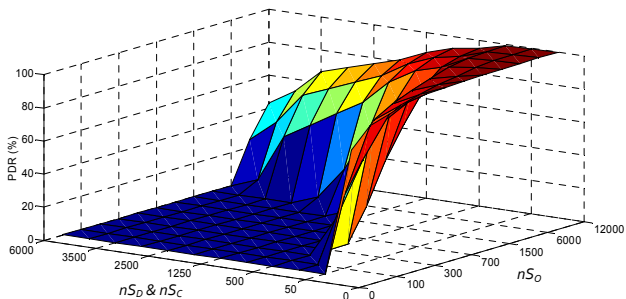


Fig. 9: PDR (transfer), Slots=1,  $S_C=2.976\text{ms}$ ,  $S_D=2.528\text{ms}$ ,  $S_O=1.004\text{ms}$

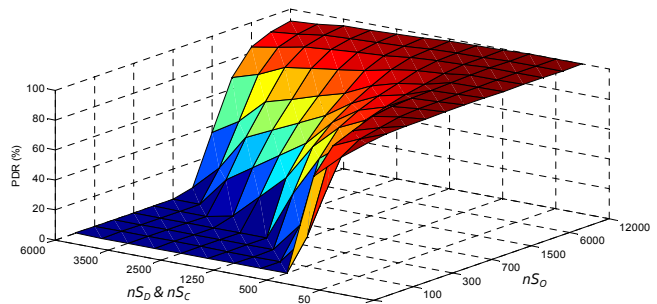


Fig. 10: PDR (transfer), Slots=8,  $S_C=2.976\text{ms}$ ,  $S_D=2.528\text{ms}$ ,  $S_O=34.208\text{ms}$

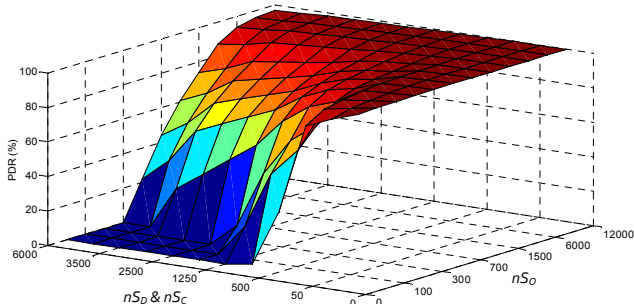


Fig. 11: PDR (transfer), Slots=20,  $S_C=2.976\text{ms}$ ,  $S_D=2.528\text{ms}$ ,  $S_O=84.576\text{ms}$

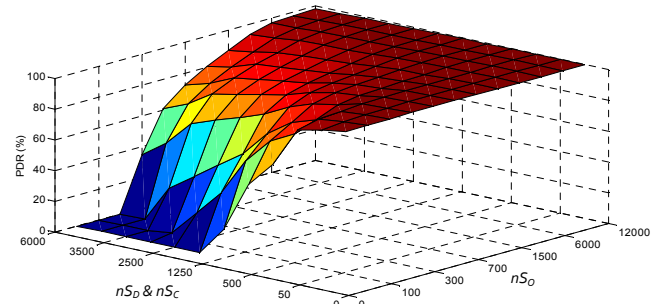
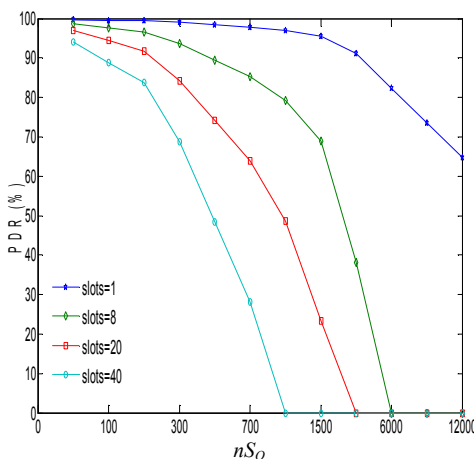
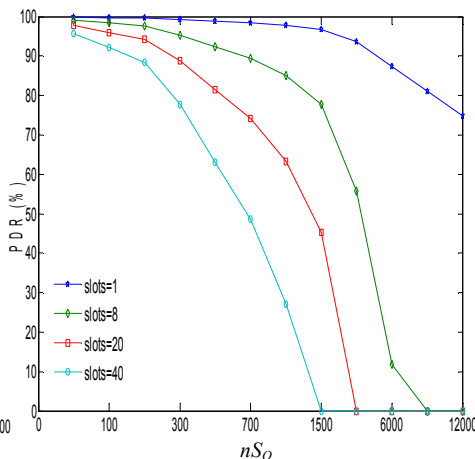


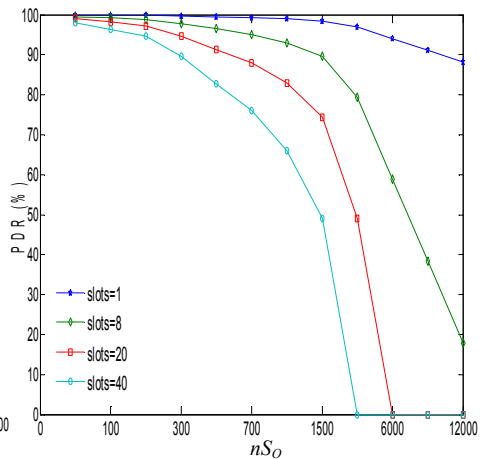
Fig. 12: PDR (transfer), Slots=40,  $S_C=2.976\text{ms}$ ,  $S_D=2.528\text{ms}$ ,  $S_O=168.48\text{ms}$



(a): Range=50m



(b): Range=70m



(c): Range=150m

Fig. 13: PDR (dissociation),  $\mathbb{E}[s]=6\text{m/s}$ ,  $\mathbb{E}[d]=9\text{m}$ ,  $\mathbb{E}[P]=6\text{s}$ ,  $n_{S_C} \& n_{S_D}=50$ ,  $S_C=2.976\text{ms}$ ,  $S_D=2.528\text{ms}$ ,

the inverse affect to its impact on the  $\text{PDR}_{transfer}$  in the case of transfer. Here, by increasing the  $nS_O$ , we are also maximizing  $SC_B$  and hence, increasing the dissociation time which will reduce the  $\text{PDR}_{dissociation}$ . Unlike in  $\text{PDR}_{transfer}$  case, here we are looking for low  $nS_O$  to ensure high  $\text{PDR}_{dissociation}$ . In addition to the  $nS_O$  value, the number of slots per superframe influences the  $\text{PDR}_{dissociation}$ , where for few slots, better  $\text{PDR}_{dissociation}$  can be achieved. This is traced to the impact of  $S_O$  on both  $SC_B$  and  $Dis$  that also maximizes dissociation time and in turn minimizes  $\text{PDR}_{dissociation}$ . Although the associated  $AST$  phase is deterministic, the remaining mobile node's lifecycle phases ( $SC_B$ ,  $AST_{req}$  and  $Dis$ ) are stochastic and thus, the impact will vary depending on the node's mobility metric.

According to Fig. 9 to Fig 13, we can deduce that both  $nS_O$  and  $S_O$  have a contradicted role in

both  $\text{PDR}_{dissociation}$  and  $\text{PDR}_{transfer}$ . Fig. 13(a) shows that for a transmission range of 50m, in order to achieve a PDR no less than 90%, the maximum number of  $nS_O$  is 150. Meanwhile, for the of case 150m, the maximum  $nS_O$  value to gain no less than 91% PDR is 500.

In order to comprehend the advantage of the proposed MA-LLDN over LLDN, Fig. 14 and 15 show how the MA-LLDN gains higher PDR than LLDN with regards to  $nS_C \& nS_D=50$ , which is considered the best scenario for LLDN. Even while varying the number of slots or transmission range, MA-LLDN exhibits different variations. This is contributed by the dependency on the  $Mgts$  inside online state to accommodate mobile node association rather than flipping to discovery and configuration states (as is the default structure of LLDN). Moreover, the flexibility of MA-LLDN to make the online

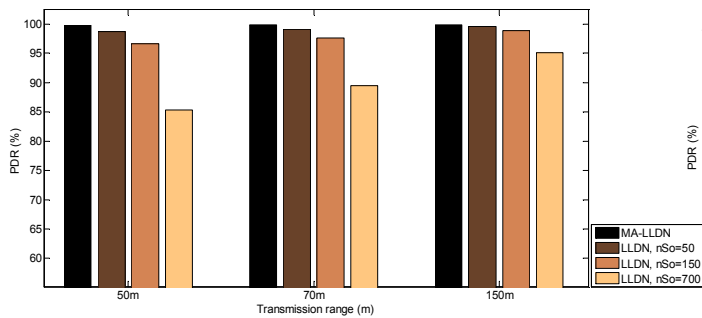


Fig. 14 : Comparison between the PDR of both LLDN and MA-LLDN, slots=8,  $S_O=34.208\text{ms}$ ,  $S_C=2.976\text{ms}$ ,  $S_D=2.528\text{ms}$ ,  $nS_C$

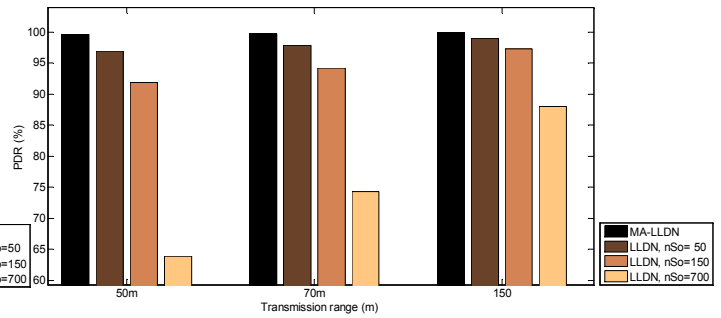


Fig. 15: Comparison between the PDR of both LLDN and MA-LLDN, slots=20,  $S_O=84.576\text{ms}$ ,  $S_C=2.976\text{ms}$ ,  $S_D=2.528\text{ms}$ ,  $nS_C=50$ .

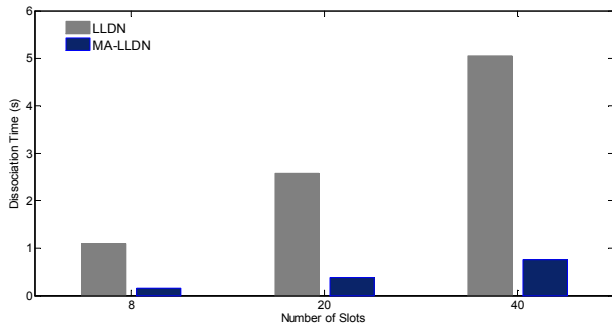


Fig. 16: Comparison between LLDN and MA-LLDN dissociation time,  $S_C=2.976\text{ms}$ ,  $S_D=2.528\text{ms}$ ,  $nS_C$  &  $nS_D$  &  $nS_O=50$ .

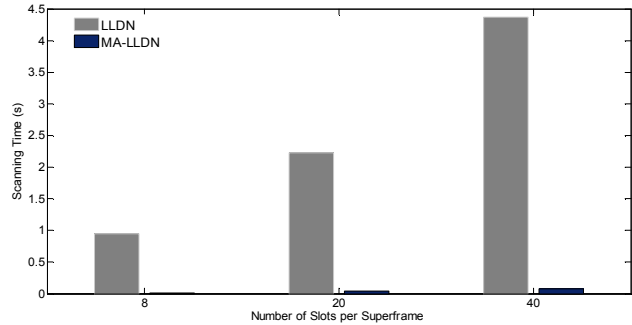


Fig. 17: Delay of scanning for beacon,  $S_C=2.976\text{ms}$ ,  $S_D=2.528\text{ms}$ ,  $nS_C$  &  $nS_D$  &  $nS_O=50$ .

state accept associations, led to ignore the impact of  $nS_C$  &  $nS_D$  on the dissociation issue.

In the meantime, to highlight the differences between MA-LLDN and LLDN in term of dissociation time, Fig. 16 depicts how the MA-LLDN manages to obtain low dissociation time while  $nS_C$  &  $nS_D$  &  $nS_O=50$ . At these settings, the LLDN has its low dissociation time (increasing these parameters will maximize the dissociation time). The most influential factor to the dissociating time is the  $SC_B$  time which is depicted in Fig 17. The  $SC_B$  is mainly affected by  $S_O$  value which is raised by increasing the number of slots in each superframe. The demonstrated dissociation time here represents the expected time that a node will be disconnected from a network once it has left a POS.

Fig. 18 describes the expected dissociated time with respect to the number of slots and  $nS_O$ . It identifies a real problem with LLDN that violates the target of low latency. It's clear that for large  $nS_O$  values the latency can be over 800s. Accordingly, to meet the required target of LLDN for  $macLLDNnumUplinkTS=20$  and a latency less than 10s, the maximum  $nS_O$  can be no greater than 200 as in Fig. 19. The realized  $PDR_{association}$  based on  $nS_O=200$  could be about 87% for 50m range and 95% for 150m range. In addition, the maximum  $PDR_{transfer}$  that can be ascertained based on these settings is 74%.

Fig. 19 shows the impact of latency incurred by dissociation versus throughput. The disadvantage at this point is that increasing  $nS_O$  here will raise rapidly the latency due to increasing the dissociation time, but in turn it has no noticeable advantage on the achieved throughput.

Finally, Fig. 20 demonstrates the relation between the  $PDR_{transfer}$  and the encountered average latency plus the ratio

of  $S_D$ ,  $S_C$  over  $S_O$ . Seeking to reduce the latency (caused by dissociation) and to achieve higher connectivity intervals, the  $nS_O$  value must be reduced against  $nS_C$  &  $nS_D$  (increasing the  $S_O$  to  $S_D$  &  $S_C$  ratio). In turn, the  $PFR_{transfer}$  is unfortunately dropping to its lowest rates of 20% and 68% for 0.81 and 0.32 ratios respectively (fixing  $nS_O$  at 100). For low  $nS_C$  value as 50, the  $PDR_{transfer}$  is rarely impacted and keeps a steady low degradation against decreasing  $nS_O$ . In summary, Fig. 20 shows the overhead of maintaining low latency on the  $PDR_{transfer}$  of the associated nodes to the network.

Fig. 21 to 23 give us a snapshot regarding the LLDN node's throughput. The case of slots=1 (i.e. just a single node exists) has not included here, but in general the average throughput to meet a dissociation of no more than 10ms is 165kbps. Fig. 21 (for slots=8) clearly shows an advantage over slots=20 and 40 since the  $S_O$  is being maximized with each slot number increase. In order to gain a dissociation less than 10ms, for the case of slots=8 and  $nS_C$  &  $nS_D=50$ , the average throughput is 23.5kbps. For the case of 20 nodes and  $nS_C$  &  $nS_D=50$ , the throughput has been declined to 9.5kbps while it has been degraded further for case of 40 nodes to be only 4.7kbps. Hence, the throughput metric must be carefully considered in order to meet the target constrains of LL applications. Regarding our analysis, we have ignored the transmission failure impact caused by packet collisions due to the fact that we assume the nodes are running with a tight synchronization that can cancel any probability of collision.

## VII. CONCLUSION

The objective of the IEEE 802.15.4e LLDN operation mode is to provide a deterministic network behavior for several application types and especially the industrial ones that require

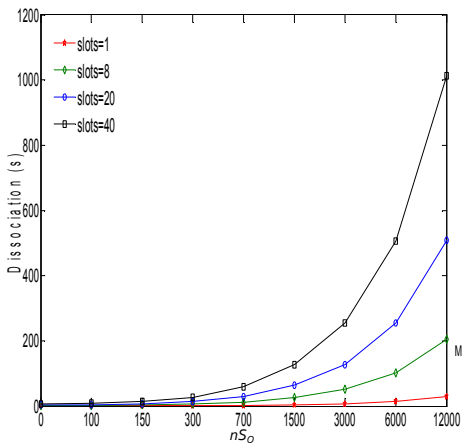


Fig. 18: Total dissociation time of LLDN,  $S_C=2.976\text{ms}$ ,  $S_D=2.528\text{ms}$ ,  $nS_C$  &  $nS_D$  &  $nS_O=50$ .

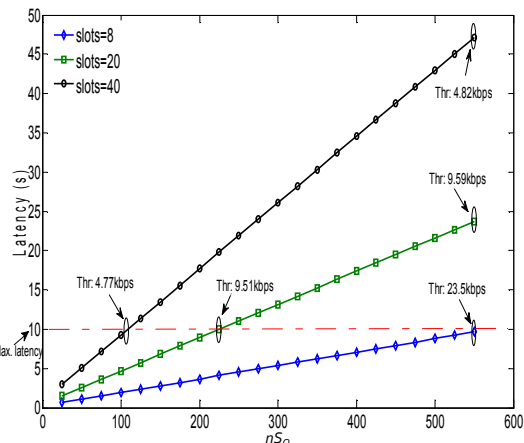


Fig. 19: Latency due to dissociation in LLDN against throughput,  $S_C=2.976\text{ms}$ ,  $S_D=2.528\text{ms}$ ,  $nS_C$  &  $nS_D=50$ .

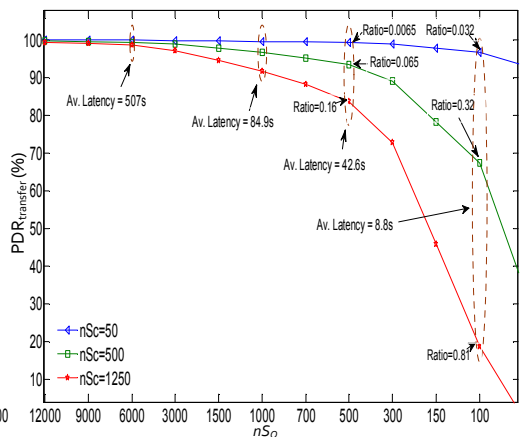


Fig. 20: PDR against  $(S_C \& S_D / S_O)$  ratio and latency due to dissociation,  $S_C=2.976\text{ms}$ ,  $S_D=2.528\text{ms}$ , slots=20

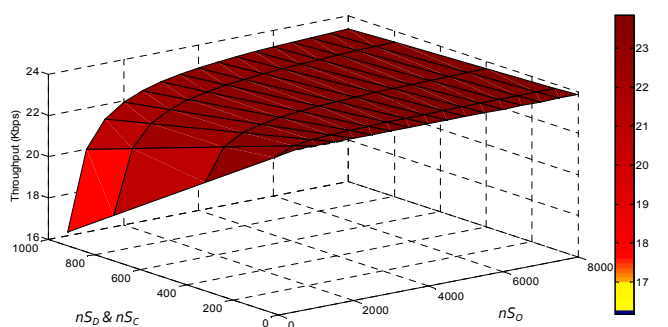


Fig. 21 : LLDN nodes throughput, slots=8,  $S_O=34.208\text{ms}$ ,  $B_F=30\text{symbols}$ ,  $\text{MSDU}=102\text{B}$ ,  $S_C=2.976\text{ms}$ ,  $S_D=2.528\text{ms}$

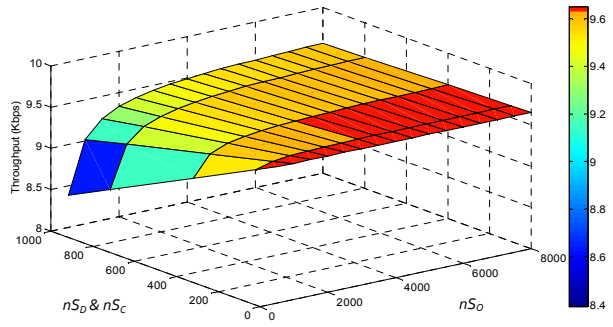


Fig. 22 : LLDN nodes throughput, slots=20,  $S_O=84.576\text{ms}$ ,  $B_F=40\text{symbols}$ ,  $\text{MSDU}=102\text{B}$ ,  $S_C=2.976\text{ms}$ ,

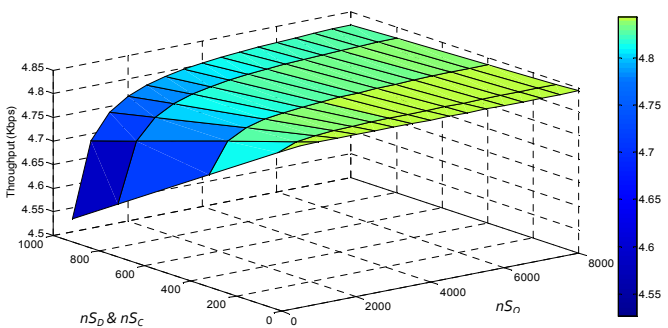


Fig. 23 : LLDN nodes throughput, slots=40,  $S_O=168.48\text{ms}$ ,  $B_F=80\text{symbols}$ ,  $\text{MSDU}=102\text{B}$ ,  $S_C=2.976\text{ms}$ ,  $S_D=2.528\text{ms}$

low latency. The determinant fact regarding several LL applications is the existence of mobile nodes, by which the default communication stack must be able to operate efficiently. Unfortunately, the default IEEE 802.15.4e LLDN infrastructure suffers with the existence of mobile nodes. Accordingly, the objective of providing deterministic and LL services has been violated. In this paper we have provided a comprehensive analysis to the impact of node mobility upon the LLDN while presenting a feasible approach to tackle the overhead of node movement. Even with a static scenario, the assumption of collecting sensor readings of 20 sensor nodes in less than 10ms is not valid unless we have no more than one byte payload, as in (3).

The major flow in the LLDN design that degrades the performance during the node movement is the classification of the network transmission status. Dividing the transmission states into three events (discovery, configuration and online) affects negatively both dissociated and associated nodes. The orphan nodes that seek to join the network are relying on both discovery and configuration transmission states to determine the network and synchronize with the coordinator. Hence, the node connectivity factor is dependent on the occurrence ratio of these two states to the duration of online states during a network lifetime. In the meantime, the throughput of the connected nodes is dependent on the interval of the online states since during the discovery and configuration states the nodes are forbidden from sending readings. Accordingly, there must be a tradeoff between the  $nS_O$  value and the value of  $nS_D$  and  $nS_C$  to realize an acceptable amount of throughput versus dissociation time. Increasing the  $nS_O$  to the value of  $nS_D$  and  $nS_C$  will maximize node throughput, but in turn increase the dissociation time.

In addition to the impact of the transmission states, the mobility metric, transmission range and superframe duration (determined by the number of slots) also influence the LLDN network functionality.

The proposed MA-LLDN model manages to reduce the dissociation time to be less than the duration of two online superframe durations. MA-LLDN reduces the dissociation delay in different scenarios by a factor of 75%. In addition, the

MA-LLDN enhances the PDR in several cases by more than 30%. In addition, MA-LLDN provides a low latency multihop structure for the LLDN mode where the readings (of nodes that are more than one hop distance) can be delivered within the same superframe. Similarly, the relay nodes can advertise passively the existence of coordinator and act accordingly as proxies to the default coordinator. Hence, MA-LLDN manages to reduce the deployment cost and the probability of overlapped beacon collisions (due to reducing the required number of coordinators). The proposed cooperative beaconing strategy between regular nodes and the coordinators has maximized the coverage area and ensures low scanning and association time and in turn, high network connectivity achieved. Finally, this paper has presented the basic metrics that must be considered prior to deploying the IEEE 802.15.4e LLDN in an environment where nodes are mobile.

#### REFERENCES

- [1] "IEEE Standard for Information technology-- Local and metropolitan area networks-- Specific requirements-- Part 15.4: Wireless Medium Access Control (MAC) and Physical Layer (PHY) Specifications for Low Rate Wireless Personal Area Networks (WPANs)," *IEEE Std 802.15.4-2006 (Revision of IEEE Std 802.15.4-2003)*, pp. 1-320, 2006.
- [2] N. Kushalnagar, G. Montenegro, and C. Schumacher, "IPv6 over low-power wireless personal area networks (6LoWPANs): overview, assumptions, problem statement, and goals," IETF, RFC 4919 2070-1721, 2007.
- [3] S. E. Deering, "Internet protocol, version 6 (IPv6) specification," *IETF, RFC 2460*, 1998.
- [4] "IEEE Standard for Local and metropolitan area networks--Part 15.4: Low-Rate Wireless Personal Area Networks (LR-WPANs) Amendment 1: MAC sublayer," *IEEE Std 802.15.4e-2012 (Amendment to IEEE Std 802.15.4-2011)*, pp. 1-225, 2012.
- [5] S. C. Mukhopadhyay, "Wearable Sensors for Human Activity Monitoring: A Review," *IEEE Sensors Journal*, vol. 15, pp. 1321-1330, 2015.
- [6] M. Becker, B.-L. Wenning, C. Görg, R. Jedermann, and A. Timm-Giel, "Logistic applications with wireless sensor networks," in *Proceedings of the 6th Workshop on Hot Topics in Embedded Networked Sensors*, 2010, p. 6.
- [7] M. Adolfsson, "A Survey on Designing Wireless Sensor Networks for Logistic Telemetry Applications," *A course in Cooperating Embedded Systems, Halmstad University, CERES*, 2005.
- [8] Z. Shelby and C. Bormann, *6LoWPAN: The wireless embedded Internet* vol. 43: John Wiley & Sons, 2011.
- [9] C. Perkins, D. Johnson, and J. Arkko, "Mobility support in IPv6," IETF, RFC 6275 2070-1721, 2011.
- [10] J. Montavont, D. Roth, and T. Noël, "Mobile ipv6 in internet of things: Analysis, experimentations and optimizations," *Ad Hoc Networks*, vol. 14, pp. 15-25, 2014.
- [11] C. Gomez, E. Kim, D. Kaspar, and C. Bormann, "Problem statement and requirements for IPv6 over low-power wireless personal area network (6LoWPAN) routing," *IETF, RFC 6606*, , 2012.
- [12] Z. Miao, Y. Yuanyuan, and W. Cong, "Mobile Data Gathering with Load Balanced Clustering and Dual Data Uploading in Wireless Sensor Networks," *IEEE Transactions on Mobile Computing*, vol. 14, pp. 770-785, 2015.
- [13] X. Guoliang, L. Minming, W. Tian, J. Weijia, and H. Jun, "Efficient Rendezvous Algorithms for Mobility-Enabled Wireless Sensor Networks," *IEEE Transactions on Mobile Computing*, vol. 11, pp. 47-60, 2012.
- [14] Z. Miao, L. Ji, and Y. Yuanyuan, "A Framework of Joint Mobile Energy Replenishment and Data Gathering in Wireless Rechargeable Sensor Networks," *IEEE Transactions on Mobile Computing*, vol. 13, pp. 2689-2705, 2014.
- [15] A. Kinalis, S. Nikolettseas, D. Patroumpa, and J. Rolim, "Biased Sink Mobility with Adaptive Stop Times for Low Latency Data Collection in Sensor Networks," in *IEEE Global Telecommunications Conference, GLOBECOM*, , 2009, pp. 1-6.
- [16] P. Ieryung, K. Dohyun, and H. Dongsoo, "MAC Achieving Low Latency and Energy Efficiency in Hierarchical M2M Networks With Clustered Nodes," *IEEE Sensors Journal*, vol. 15, pp. 1657-1661, 2015.
- [17] M. Arifuzzaman, M. Matsumoto, and T. Sato, "An Intelligent Hybrid MAC With Traffic-Differentiation-Based QoS for Wireless Sensor Networks," *IEEE Sensors Journal*, vol. 13, pp. 2391-2399, 2013.
- [18] M. Bagaa, M. Younis, D. Djenouri, A. Derhab, and N. Badache, "Distributed Low-Latency Data Aggregation Scheduling in Wireless Sensor Networks," *ACM Transactions on Sensor Networks (TOSN)*, vol. 11, p. 49, 2015.
- [19] N. Duc-Long, T. Le Quang Vinh, O. Berder, and O. Sentieys, "A low-latency and energy-efficient MAC protocol for cooperative wireless sensor networks," in *IEEE Global Communications Conference (GLOBECOM)*, , 2013, pp. 3826-3831.
- [20] A. Berger, M. Pichler, W. Haslmayr, and A. Springer, "Energy Efficient and Reliable Wireless Sensor Networks-An Extension to IEEE 802.15. 4e," *EURASIP Journal on Wireless Communications and Networking 2014*, 2014:126 doi:10.1186/1687-1499-2014-126, 2014.
- [21] A. Berger, A. Entinger, A. Potsch, and A. Springer, "Improving IEEE 802.15.4e LLDN performance by relaying and extension of combinatorial testing," in *IEEE Emerging Technology and Factory Automation (ETFA)*, , 2014, pp. 1-4.
- [22] E. Uhlemann and A. Willig, "Joint Design of Relay and Packet Combining Schemes for Wireless Industrial Networks," in *IEEE Vehicular Technology Conference, VTC Spring*, 2008, pp. 2441-2445.
- [23] G. Patti, G. Alderisi, and L. L. Bello, "Introducing multi-level communication in the IEEE 802.15.4e protocol: The MultiChannel-LLDN," in *IEEE Emerging Technology and Factory Automation (ETFA)*, , 2014, pp. 1-8.
- [24] L. Dariz, G. Malaguti, and M. Ruggeri, "Performance analysis of IEEE 802.15.4 real-time enhancement," in *IEEE 23rd International Symposium on Industrial Electronics (ISIE)*, , 2014, pp. 1475-1480.
- [25] M. Anwar and Y. Xia, "IEEE 802.15.4e LLDN: Superframe configuration for networked control systems," in *33rd Chinese Control Conference (CCC)*, , 2014, pp. 5568-5573.
- [26] H. Kapil and C. S. R. Murthy, "Rainbow product ranking based relay placement and adaptive retransmission scheme for a reliable 802.15.4e LLDN," in *IEEE International Conference on Industrial Technology (ICIT)*, , 2015, pp. 1914-1919.
- [27] F. Qinyuan, H. Kai, and D. Yafei, "Rainbow Product Ranking for Upgrading E-Commerce," *IEEE Internet Computing*, vol. 13, pp. 72-80, 2009.
- [28] R. C. Larson and A. R. Odoni, *Urban operations research*: Prentice Hall, Englewood Cliffs, NJ, 1981.
- [29] D. P. Bertsekas and J. N. Tsitsiklis, *Introduction to Probability*: Athena Scientific, Second Edition, 2008.
- [30] F. Bai and A. Helmy, "A survey of mobility models," *Wireless Adhoc Networks. University of Southern California, USA*, vol. 206, 2004.
- [31] P. Johansson, T. Larsson, N. Hedman, B. Mielczarek, and M. Degermark, "Scenario-based performance analysis of routing protocols for mobile ad-hoc networks," in *Proceedings of the 5th annual ACM/IEEE international conference on Mobile computing and networking*, 1999, pp. 195-206.
- [32] N. Bulusu, D. Estrin, L. Girod, and J. Heidemann, "Scalable coordination for wireless sensor networks: self-configuring localization systems," in *International Symposium on Communication Theory and Applications (ISCTA 2001)*, Ambleside, UK, 2001.
- [33] C. Bettstetter, H. Hartenstein, and X. Pérez-Costa, "Stochastic properties of the random waypoint mobility model," *Wireless Networks*, vol. 10, pp. 555-567, 2004.
- [34] S. Bandyopadhyay, E. J. Coyle, and T. Falck, "Stochastic Properties of Mobility Models in Mobile Ad Hoc Networks," *IEEE Transactions on Mobile Computing*, vol. 6, pp. 1218-1229, 2007.

- [35] E. L. Kaplan and P. Meier, "Nonparametric estimation from incomplete observations," *Journal of the American statistical association*, vol. 53, pp. 457-481, 1958.
- [36] W. Dalei, C. Song, W. Haohong, and A. K. Katsaggelos, "Application-Centric Routing for Video Streaming Over MultiHop Wireless Networks," *IEEE Transactions on Circuits and Systems for Video Technology*, vol. 20, pp. 1721-1734, 2010.
- [37] I. F. Akyildiz, T. Melodia, and K. R. Chowdury, "Wireless multimedia sensor networks: A survey," *IEEE Wireless Communications*, vol. 14, pp. 32-39, 2007.
- [38] C. Buratti, "Performance Analysis of IEEE 802.15.4 Beacon-Enabled Mode," *IEEE Transactions on Vehicular Technology*, vol. 59, pp. 2031-2045, 2010.
- [39] K. Jin-Woo, K. Jihoon, and E. Doo-Seop, "Multi-dimensional channel management scheme to avoid beacon collision in LR-WPAN," *IEEE Transactions on Consumer Electronics*, vol. 54, pp. 396-404, 2008.
- [40] N. Nordin and F. Dressler, "Effects and Implications of Beacon Collisions in Co-Located IEEE 802.15.4 Networks," in *IEEE Vehicular Technology Conference (VTC Fall)*, 2012, pp. 1-5.
- [41] E. Toscano and L. Lo Bello, "A multichannel approach to avoid beacon collisions in IEEE 802.15.4 cluster-tree industrial networks," in *IEEE Conference on Emerging Technologies & Factory Automation, ETFA*, 2009, pp. 1-9.
- [42] Y. Al-Nidawi, S. Naveed, and A. H. Kemp, "Mesh-Under Cluster-Based Routing Protocol for IEEE 802.15.4 Sensor Network," in *Proceedings of 20th European Wireless Conference*, 2014, pp. 1-7.
- [43] Z. Hanzalek and P. Jurcik, "Energy Efficient Scheduling for Cluster-Tree Wireless Sensor Networks With Time-Bounded Data Flows: Application to IEEE 802.15.4/ZigBee," *IEEE Transactions on Industrial Informatics*, vol. 6, pp. 438-450, 2010.
- [44] A. Koubaa, R. Severino, M. Alves, and E. Tovar, "Improving Quality-of-Service in Wireless Sensor Networks by Mitigating Hidden-Node Collisions," *IEEE Transactions on Industrial Informatics*, vol. 5, pp. 299-313, 2009.
- [45] S. Shiann-Tsong, S. Yun-Yen, and L. Wei-Tsong, "CSMA/CF Protocol for IEEE 802.15.4 WPANs," *IEEE Transactions on Vehicular Technology*, vol. 58, pp. 1501-1516, 2009.